THESIS

MECHANICAL STUDIES OF CADMIUM SULFIDE/CADMIUM TELLURIDE (CdS/CdTe) PHOTOVOLTAIC MODULES

Submitted by

Mark Andrew Armijo

Department of Mechanical Engineering

In partial fulfillment of the requirements

For the Degree of Master of Science

Colorado State University

Fort Collins, Colorado

Summer 2015

Master's Committee:

Advisor: Walajabad Sampath

Donald Radford
James Sites

ABSTRACT

MECHANICAL STUDIES OF CADMIUM SULFIDE/CADMIUM TELLURIDE (CdS/CdTe) PHOTOVOLTAIC MODULES

Commercial Cadmium Sulfide (CdS) and Cadmium Telluride (CdTe) photovoltaic modules are typically 24" x 48". The processing steps include: glass heating, Cadmium Sulfide (CdS) deposition and Cadmium Telluride (CdTe) deposition, Cadmium Chloride ($CdCl_2$) heat treatment, back contact formation and back contact heat-treatment. The main components of the photovoltaic module under consideration in this research are the tempered front glass, an encapsulant (ethylene vinyl acetate (EVA)) interlayer, and the tempered bottom glass. During processing, the front glass loses a certain degree of temper. This results in the reduction of the residual stress within the front glass and ultimately reduces the strength of the module. The residual stress before and after processing was measured. The glass heating reduced the residual stress from 10,000 psi to approximately 2,500 psi. Even with the loss of the residual stress, the modules passed the static load test of 2,400 Pa and survived the hail impact test (1" ice balls at 50 mph). The mechanical behavior of the composite photovoltaic (PV) modules under static mechanical load and hail impact load utilizing mechanics modeling and experimental testing were characterized. The accuracy of the theoretical model is compared to the results of the experimental testing. The results will provide valuable knowledge for the mechanical characteristics of the PV module. This will contribute to the understanding of the effects of temper loss and whether the module exhibits a loss in strength.

ACKNOWLEDGEMENTS

I would like to thank my advisor, Dr. Walajabad S. Sampath, for all his guidance, patience and assistance throughout the completion of my Master's degree. I would also like to thank the members of my graduate committee, Dr. James R. Sites and Dr. Donald Radford for providing their suggestions and advice.

I would also like to thank my group management at Los Alamos National Laboratory (Derrick Montoya, Frank Garcia) for supporting me in taking a leave of absence to complete my degree.

I want to thank the Graduate Engineering Minority (GEM) Fellowship for the provided financial support. As well as Dr. Omnia Hakim for providing financial assistance through the PEAKS program at CSU. I would also like to thank Bill Blumenthal and Manny Lovato who provided testing support at Los Alamos National Laboratory. I would like to thank my wife, Brenda and two children, Kaitlyn and Ethan for their undying support.

DEDICATION

I would like to dedicate the efforts put forth in the thesis to my wife Brenda, daughter Kaitlyn and son Ethan. Without their constant support and encouragement this work would not have been possible.

TABLE OF CONTENTS

LIST OF TABLES

LIST OF FIGURES

Chapter 1: INTRODUCTION

1.1. Photovoltaic Applications and the Growth of the Industry

Solar cells, otherwise known as photovoltaics (PV), convert sunlight directly into electricity. They are manufactured from semiconducting materials. When sunlight is absorbed by these devices, the solar energy creates electron hole pairs allowing the charge carriers to flow through the material to produce electricity. This process of converting light (photons) to electricity is known as the photovoltaic effect. Thin film solar cells use layers of semiconducting materials that are only micrometers thick

The increased energy needs throughout the world has increased the importance and interest in renewable energy sources such as photovoltaic solar cells. World production of PV modules has increased at the rate of 35% per year, from 88.6 MW in 1996 to approximately 39 GW currently. [Jäger-Waldau, 2013]. Increasing efficiency and reducing cost is necessary to expand the use of PV.

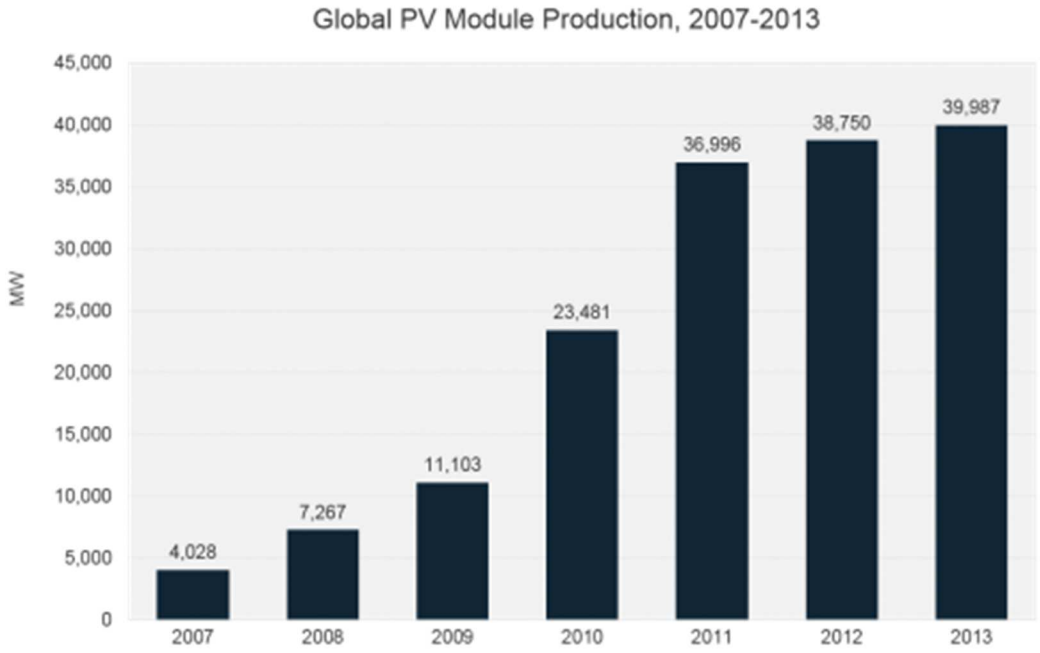

Figure 1 – Global PV Production [GTM Research, 2014]

1.2. Processing of Photovoltaic Modules

There is ongoing research occurring at the Materials Engineering Laboratory (MEL) at Colorado State University in the area of mass production of thin film Cd/CTe photovoltaic (PV) modules. The current process exists in a continuous, all in-line system where all manufacturing steps are performed in one vacuum boundary. These processing steps include glass heating, Cadmium Sulfide (CdS) and Cadmium Telluride (CdTe) deposition, Cadmium Chloride ($CdCl_2$) heat treatment, back contact formation and back contact heat-treatment [Sampath, 2004]. The schematic of the pilot manufacturing system is shown in Figure 2.

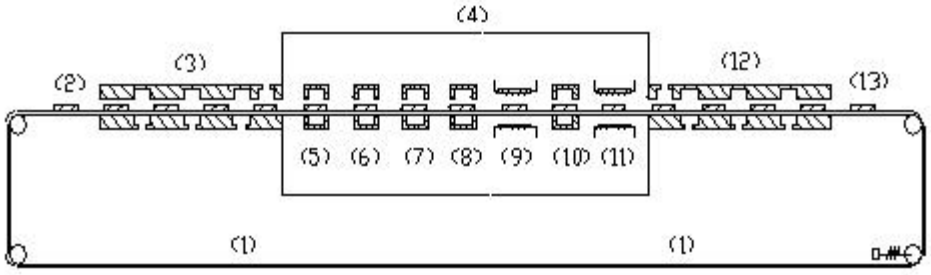

Schematic of the Pilot System for CdTe PV Fabrication (1) belt conveyor, (2) glass substrate, (3) air to vacuum to air (AVA) seal, (4) vacuum chamber, (5) heating module, (6) CdS deposition, (7) CdTe deposition, (8) CdCl2 deposition and heat treatment, (9) CdCl2 annealing and stripping, (10) ohmic contact formation, (11) contact annealing, (12) AVA seal, (13) completed cell

Figure 2 - Schematic of PV Manufacturing Process

A patented process for manufacturing CdS/CdTe modules includes the following steps: 1) cleaning the transparent conductive oxide (TCO) coated glass substrates, 2) heating the substrates, 3) depositing n-type CdS layer, 4) depositing p-type CdTe layer, 5) performing a $CdCl_2$ treatment to improve CdTe grain structure and electrical properties, 6) forming a p+ ohmic low resistance contact layer to improve current collection from the CdTe, 7) depositing a metal layer (metallization) to form the back electrode, 8) scribing the film layers into individual cells, 9) interconnecting the cells in series and providing a means of electrical connection to the module, and 10) encapsulating the finished module.

Tempered glass is used to increase the strength of the module. However, the heating of the glass during the manufacturing of the PV module reduces the residual stress. The aim of this thesis is to investigate the effect of the loss of residual stress on the strength of the module.

The technology uses a continuous-belt conveyor to transport the glass substrates from air to vacuum and then back to air. Heated-pocket deposition is a proprietary vapor-source technology for efficient deposition of metals or compounds in vacuums with a high degree of

film uniformity. A unique substrate-heating technology allows rapid heating of substrates in vacuum to a high temperature with excellent thermal uniformity without inducing thermal stress. A photograph of the prototype PV production equipment located at the MEL at CSU is shown in Figure 3. Substrate-temperature uniformity is critical in achieving film-thickness uniformity and properties. Using this technology, 12.8% efficient devices have been produced and verified by the National Renewable Energy Laboratory (NREL). Recently efficiencies of 16.4% have been demonstrated.

Figure 3 – Prototype PV Production Equipment

All PV modules must undergo qualification testing to evaluate modules for their design performance, safety and susceptibility to known failure mechanisms. Certain test standards specify a common approach to conduct qualification testing. For the thin film flat plate modules manufactured at the MEL, IEEE 1262 *(IEEE Recommended Practice for Qualification of Photovoltaic (PV) Modules),* IEC 61215 *(Design Qualification and Type Approval for*

Crystalline Silicon Terrestrial Photovoltaic Modules) and IEC 61646 *(Thin Film Torrential Photovoltaic (PV) Modules - Design Qualification and Type Approval)* define the required tests, test procedures and pass criteria. The scope of this thesis is to expand on previous research to characterize the mechanical behavior of a CdS/CdTe PV module under static mechanical load and hail impact load utilizing mechanics modeling and experimental testing.

The guidance specified in these test standards will be used to study the static mechanical load characteristics and the hail impact loading characteristics. Classic mechanics of materials equations have been used to analyze the mechanical loading and stress effects on the composite layers within the module. [Appendix A] The knowledge gained from the stress analysis will assist researchers in determining the useful life of a PV module under certain environmental conditions.

1.3. Problem Description

This study will characterize the mechanical behavior of a CdS/CdTe photovoltaic (PV) module under static mechanical load and hail impact load utilizing mechanics modeling and experimental testing. The guidance for the testing is set forth in the IEEE 1262 Standard. For the mechanical loading tests, the test is meant to simulate static and dynamic loading caused by wind or snow loading. The required static load is 2400 Pa (50 lb/ft^2).

For hail impact, the intent is to determine whether the module can withstand a simulated hail impact without undergoing any damage.

Chapter 2: LITERATURE REVIEW

2.1 Review of Existing Literature

The focus of the literature review is to determine the available knowledge and research that may exist in the area of mechanical behavior for a glass composite plate structure. The initial investigation into the literature has resulted in various research studies pertaining to composite glass structures.

Information related to laminates under uniform pressure provides guidance in understanding the deformation and fracture behavior of a glass laminate. There are notable differences between monolithic glass and laminate glass fracture which typically consists of three sequential events: 1) first cracking in one glass ply, 2) rapid fragmentation of both glass plies, and 3) stretching and ultimate rupture of the polymer interlayer with associated interfacial debonding. However, the majority of testing reported has covered a narrow range of temperature, loading rate, specimen sizes, and shape and little attention has been paid to the sequence of fracture development [Van Duser, 1999].

Various articles analyze laminated glass (LG) consisting of two or more glass plies bonded together with an elastomeric interlayer, usually polyvinyl butyral (PVB) [Norville, 1998]. Laminated glass is mostly found in automobile vehicle windshields. When the laminated glass breaks, it usually holds resultant shards together and for the most part the laminated glass remains in the frame. This breakage characteristic provides substantial safety in accidents.

Norville *et al* modeled laminated glass as a simply supported beam with two glass plies each have thickness s and a PVB interlayer of thickness t. The beam has a length L and unit width containing a uniform load of magnitude w along the length of the beam. (See Figure 4)

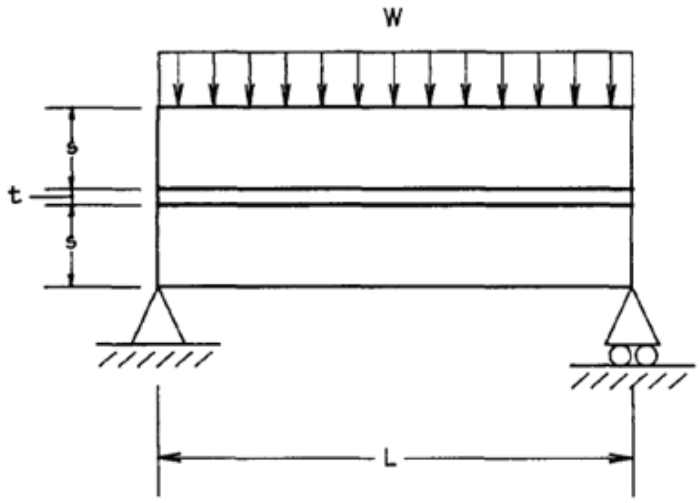

Figure 4 – Laminate Glass Beam [Norville, 1998]

Norville also defined certain bounds which characterize laminated glass behavior. Figure 5 and Figure 6 show the flexural stress distributions for the bounding models [Norville, 1998]. In the upper bound model shown in Figure 5, all layers act together as one beam. In Figure 6, the lower bound model, the layers act as three separate beams. If the upper bound model (top boundary condition) exists, the flexural stress in the top glass ply would be entirely compressive and the flexural stress in the bottom glass ply would be entirely tensile. The model in the work performed by Norville *et al* assume that the PVB performs no functions other than maintaining spacing between the glass plies and transferring a fraction of the horizontal shear force between the glass plies.

In testing the PV modules, the research goal was to determine whether the layers behave together as one beam or as two separate beams. The calculated and measured maximum deflections values in the center loaded PV module will be compared in order to understand the beam deflection behavior.

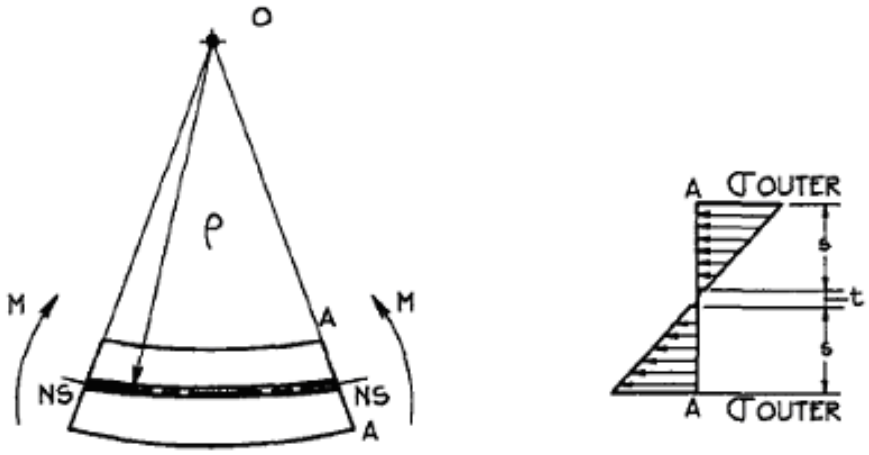

Figure 5 - Flexural Stress Distributions, Upper Bound Model [Norville, 1998]

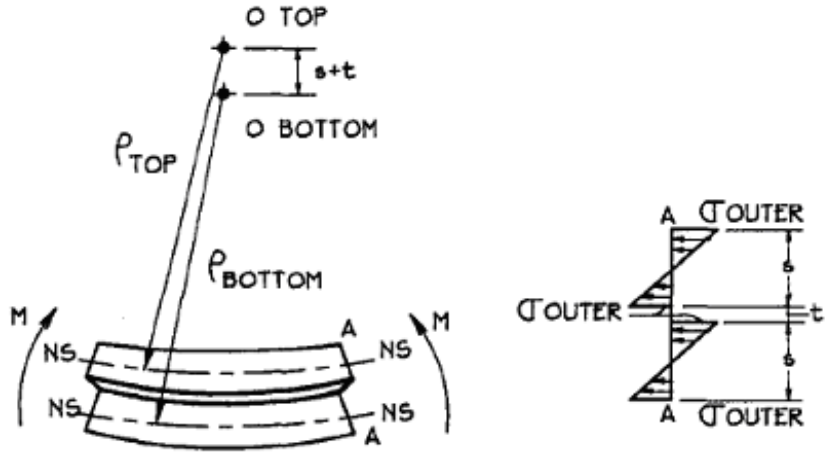

Figure 6 - Flexural Stress Distributions, Lower Bound Model [Norville, 1998]

Research investigations performed by Flocker and Dharani consider the stresses in laminated glass due to low velocity impact [Flocker, 1997]. The analysis models two glass plies separated with PVB. A spherical chromium steel ball was used to model the initial impact velocity. The main focus of the research is to determine the stresses at the surface of the glass plies. The surface is the typical location where cracks tend to open and propagate under tensile stress.

The literature review has found several research areas with associated information that can potentially be used in modeling the PV module. One area to further investigate is the

correlation between PVB and ethylene vinyl acetate (EVA). PVB is considered to be a viscoelastic polymer. The properties of this material must be compared with EVA encapsulant that is currently used in the composite PV modules.

Chapter 3: METHOD OF ANALYSIS

In order to research the stress analysis in a photovoltaic module, it is necessary to make several assumptions. This includes the loading characteristics applied to the composite structure and any boundary conditions that may be relevant. For our purposes, the hail impact will be modeled as a 1" diameter ice sphere exerting a single point load in the center of the PV module with a value of 672 lb_f for a time of 57.4 μs. This is a calculated force assuming constant acceleration of 398,212 m/s^2. [Appendix B]. In addition, it is assumed no debonding exists between the EVA and the glass layers. The calculated and measured maximum deflections values in the center loaded PV module correspond to single beam deflection behavior. The applied thin film deposition of CdS and CdTe can be considered negligible for stress analysis purposes.

The glass transition of EVA as measured using dynamic mechanical analysis, begins at temperatures of about -15 °C. Because of increased moduli below the glass transition temperature, a module may be more vulnerable to damage if a mechanical load is applied by snow or wind at low temperatures. [Kempe, 2006]. Since the EVA is a crosslinked polymer there is no viscoelastic deformation. For this research, all tests and measurements were performed at ambient temperatures.

A generic top view of the PV module is shown in Figure 7. A side view of the photovoltaic composite structure is shown in Figure 8. The tempered and untempered soda lime glass layers each have a thickness of 3 mm (0.118"). The EVA encapsulant has a thickness of 0.5 mm (0.0196").

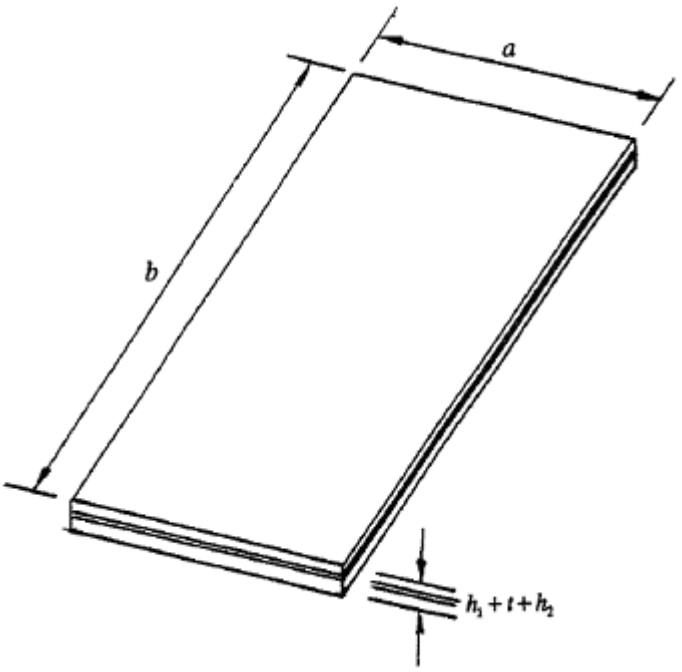

Figure 7 – Generic Top View of PV Module

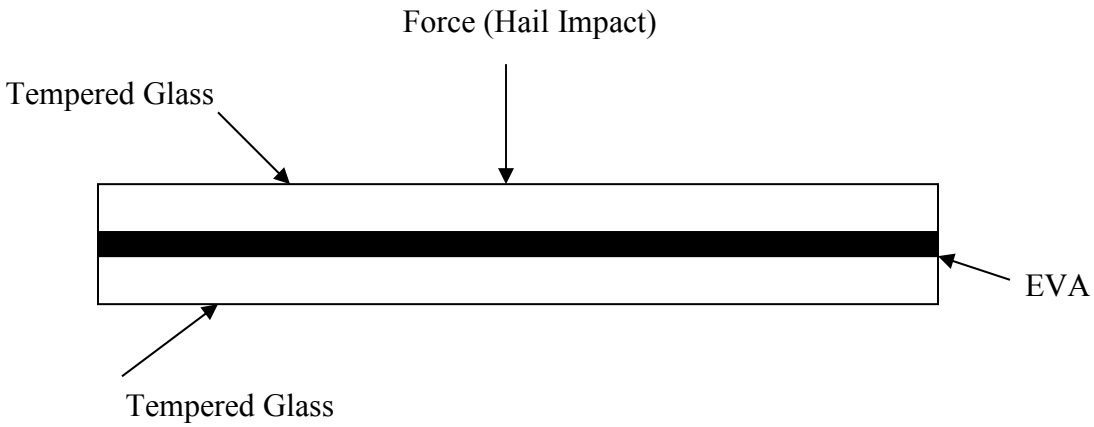

Figure 8 - Side View of PV Module

When impacted by hail, the composite structure will bend and exhibit compression forces where the hail impacts the tempered front glass plate and tension forces on the untempered back plate glass. There will be Hertzian contact stresses and some of the Hertzian contact stresses will be tensile. The encapsulant layer will exhibit stress characteristics within the composite

structure. Depending on the thickness of the EVA, the composite may behave as one beam in bending or as two separate beams in bending.

In performing the mathematical analysis, several classic mechanics of materials equations are utilized. Equation 1 will obtain the maximum normal stress, assuming Hooke's law applies where the normal stress (σ_y) does not exceed the yield strength (σ_y). Equation 2 will obtain the maximum shearing stress in a given section of a narrow rectangular beam. Equation 3 will obtain strain values within the composite layers.

$$\sigma = \frac{Mc}{I} \quad (1) \qquad \tau_{\max} = \frac{3V}{2A} \quad (2) \qquad \varepsilon = \frac{\sigma}{E} \quad (3)$$

Actual testing of PV modules in the laboratory will provide verification of the mathematical model. When these formulas are applied to the single beam, it assumes no relative motion between the glass/EVA/glass module.

Chapter 4: EXPERIMENTAL DESIGN

4.1 Introduction

The experimental design will consist of a testing scenario that will simulate static and dynamic mechanical loading typical of wind or snow loading. For the static load testing, the setup includes placing (4)-twenty pound sandbags over the module to determine the amount of deflection. The sandbags simulate the requirement of an essentially uniform load of 2400 Pa being applied normal to the module surface. The weight of the sandbags (80 pounds) divided by the area of the module (1.60 ft^2) results in a load of 49.87 lbf/ft^2 (2387.78 Pa). A cycle consisted of leaving the sandbags in place for 30 minutes for the topside deflection measurement. The load was then removed and reapplied to the opposite surface for 30 minutes for the backside deflection measurement. The requirement from IEEE 1262 states: "An essentially uniform load of 2400 Pa should be applied normal to the module surface and left in place for 30 min. The load should be removed and reapplied to the opposite surface for 30 min. These two loadings should be repeated for three cycles." The two loadings were repeated for three cycles with deflection measurements taken before and after the loadings. The modules were fastened on both ends. Measurements were taken using a calibrated micrometer at the center edge of each PV module. For the topside deflection, results ranged from a minimum of 0.0160 in. (0.4064 mm) to a maximum of 0.0550 in. (1.397 mm). For the backside deflection, results ranged from a minimum of 0.0095 in. (0.2413 mm) to a maximum of 0.0520 in. (1.321 mm). More rigid supports during the sandbag testing are required in order to perform a statistics analysis that would determine if the difference in the topside and backside deflection measurements is statistically significant. The rigid supports would also be required to determine any existence of permanent deflection (residual deflection) due to sandbag testing.

Table 1 - Deflection Measurements from Sandbag Testing

Cycle	Top Glass	Back Glass	Topside Deflection			Backside Deflection		
			Before (in.)	After (in.)	Delta (in.)	Before (in.)	After (in.)	Delta (in.)
1	T/P #1	BG #3	1.0440	1.0040	0.0400	1.0300	1.0110	0.0190
2	T/P #1	BG #3	1.0010	0.9750	0.0260	1.0130	0.9840	0.0290
3	T/P #1	BG #3	0.9800	0.9565	0.0235	0.9860	0.9625	0.0235
1	T/P #2	BG #4	0.9885	0.9665	0.0220	0.9820	0.9540	0.0280
2	T/P #2	BG #4	0.9975	0.9700	0.0275	0.9720	0.9440	0.0280
3	T/P #2	BG #4	0.9645	0.9480	0.0165	0.9630	0.9520	0.0110
1	T/P #4	BG #4	0.9885	0.9665	0.0220	0.9820	0.9540	0.0280
2	T/P #4	BG #4	0.9975	0.9700	0.0275	0.9720	0.9440	0.0280
3	T/P #4	BG #4	0.9645	0.9480	0.0165	0.9630	0.9520	0.0110
1	T/P #5	BG #5	0.9750	0.9510	0.0240	1.0200	0.9950	0.0250
2	T/P #5	BG #5	1.0040	0.9875	0.1650	0.9650	0.9430	0.0220
3	T/P #5	BG #5	1.0080	0.9650	0.0430	0.9700	0.9450	0.0250
1	UT #11 (w/TCO)	BG #11	1.0130	0.9850	0.0280	1.000	0.9860	0.0140
2	UT #11 (w/TCO)	BG #11	1.0240	0.9955	0.0285	1.0010	0.9770	0.0240
3	UT #11 (w/TCO)	BG #11	1.0280	0.9940	0.0340	0.9950	0.9830	0.0120
1	UT #10 (w/TCO)	BG #10	0.9940	0.9700	0.0240	0.9790	0.9650	0.0140
2	UT #10 (w/TCO)	BG #10	1.0300	1.0040	0.0260	1.0110	0.9800	0.0310
3	UT #10 (w/TCO)	BG #10	0.9805	0.9525	0.0280	1.0080	0.9870	0.0210
1	UT #9 (w/TCO)	BG #9	0.9800	0.9620	0.0180	1.0140	0.9850	0.0290
2	UT #9 (w/TCO)	BG #9	1.0150	0.9860	0.0290	1.0040	0.9810	0.0230
3	UT #9 (w/TCO)	BG #9	0.9955	0.9760	0.0195	0.9885	0.9650	0.0235
1	UT #8 (w/TCO)	BG #8	0.9890	0.9730	0.0160	0.9880	0.9700	0.0180
2	UT #8 (w/TCO)	BG #8	0.9835	0.9580	0.0255	0.9925	0.9660	0.0265
3	UT #8 (w/TCO)	BG #8	0.9985	0.9750	0.0235	0.9730	0.9520	0.0210

1	UT #7 (w/TCO)	BG #7	0.9805	0.9475	0.0330	0.9870	0.9545	0.0325
2	UT #7 (w/TCO)	BG #7	0.9690	0.9385	0.0305	1.0045	0.9855	0.0190
3	UT #7 (w/TCO)	BG #7	0.9760	0.9445	0.0315	1.0115	0.9735	0.0380
1	UT #6 (w/TCO)	BG #6	0.9975	0.9740	0.0235	0.9900	0.9615	0.0285
2	UT #6 (w/TCO)	BG #6	0.9945	0.9720	0.0225	0.9845	0.9655	0.0190
3	UT #6 (w/TCO)	BG #6	0.9995	0.9770	0.0225	0.9730	0.9590	0.0140
1	UT #1	BG #2	1.0030	0.9745	0.0285	1.0022	0.9680	0.0342
2	UT #1	BG #2	1.0005	0.9740	0.0265	0.9980	0.9755	0.0225
3	UT #1	BG #2	1.0020	0.9785	0.0235	0.9930	0.9740	0.0190
1	UT #2	BG #1	0.9730	0.9535	0.0195	0.9875	0.9675	0.0200
2	UT #2	BG #1	0.9775	0.9530	0.0245	0.9980	0.9805	0.0175
3	UT #2	BG #1	1.0065	0.9845	0.0220	1.0080	0.9875	0.0205
				MAX	**0.0550**		**MAX**	**0.0520**
				MIN	**0.0160**		**MIN**	**0.0095**
				AVE	**0.0270**		**AVE**	**0.0228**

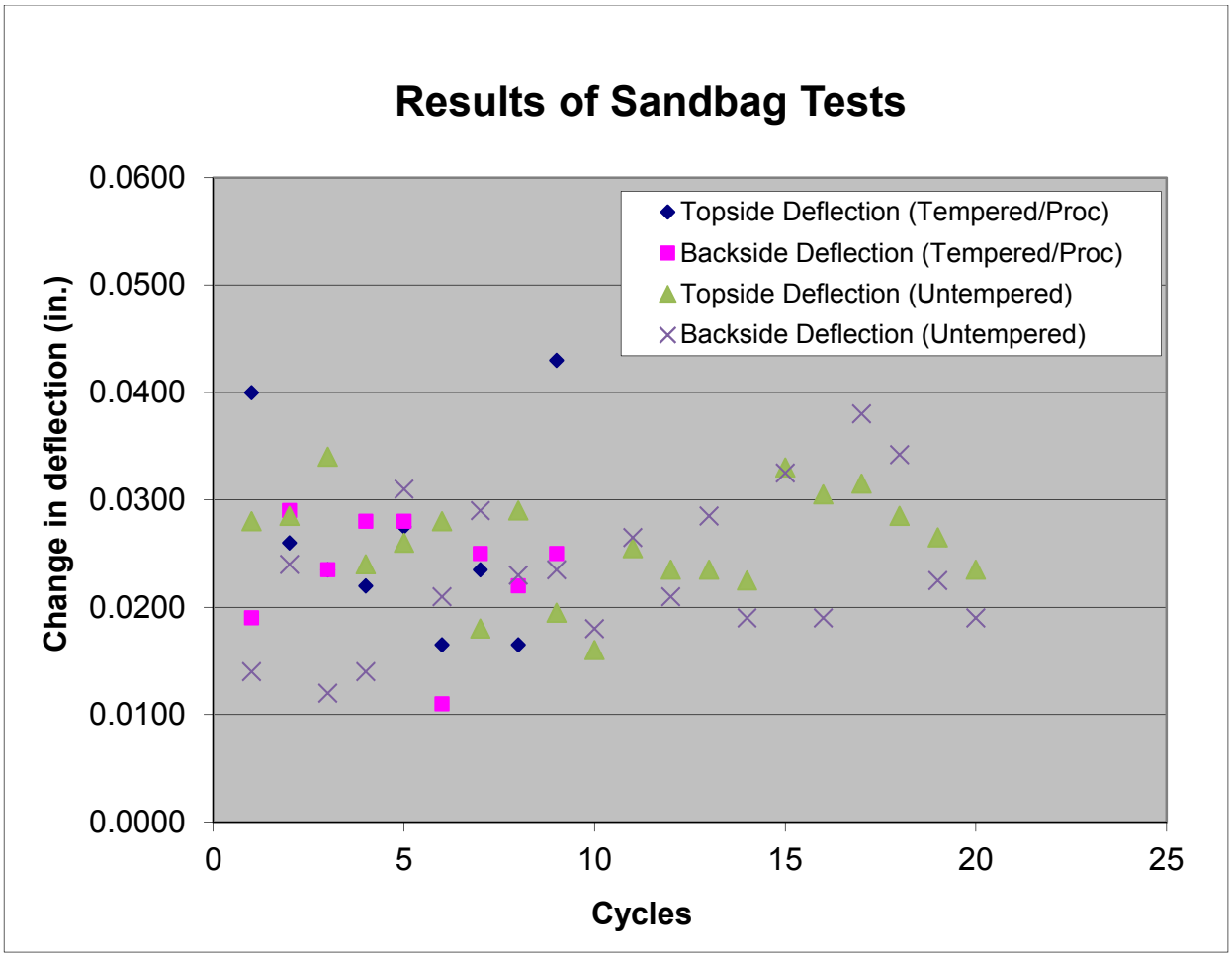

Figure 9 - Results of Sandbag Testing

Each module passed the visual inspection requirements as specified by IEEE 1262 standard. The results are tabulated in Table 1 and a graphical representation is shown in Figure 9. A photograph of the configuration for the sandbag test is shown in Figure 10. The results of the sandbag testing demonstrate that the loss of residual stress during processing does not decrease the strength of the module to levels that are not acceptable.

Figure 10 – Sandbag Testing Configuration

A Los Alamos National Laboratory (LANL) owned MTS Instron machine with a 0.01 – 500 mm/min rate of travel and maximum travel of 200 mm was used for the load testing. The equipment was located at a center point of the PV module with supports at 1.125" from each end to simulate installation. The configuration is shown in Figure 11. The equipment's calibration schedule was current during the testing operations. The loading rate for all testing was established at 1 mm/min.

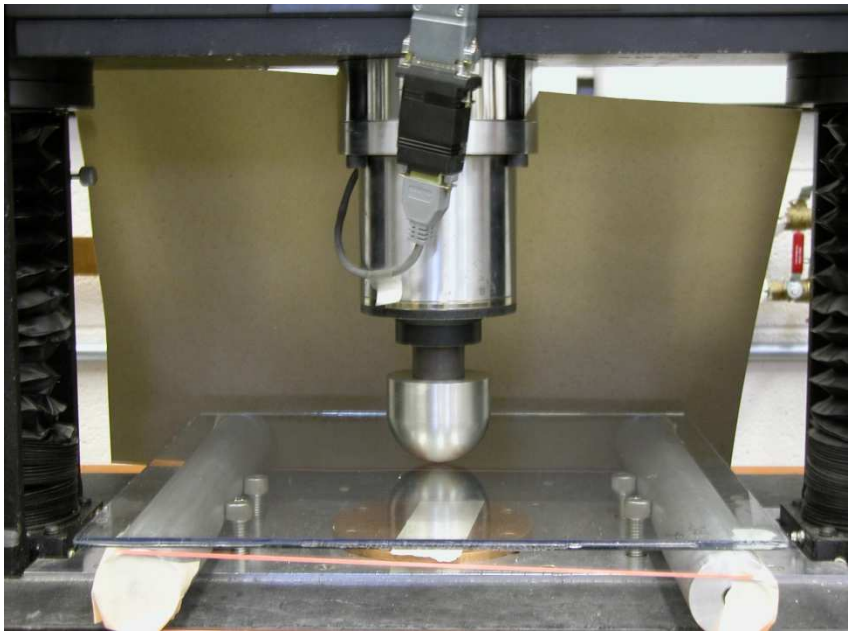

Figure 11 – Load Testing Configuration

Load testing with the Instron machine was performed on ten samples. Two samples were tempered and had been processed through the glass heating stage of the air-to-vacuum to air (AVA) manufacturing process. The remaining eight samples were untempered and had not been processed through the glass heating stage. The two tempered/processed samples that had been heat strengthened in the glass heating stage were loaded to fracture with the resulting peak loads at 4018 N and 3604 N. Load testing results are shown in Table 2. The load testing with the Instron machine is not a requirement for the PV module qualification testing. The testing was performed to determine the amount of deflection the modules exhibited. It was also performed to determine if tempered/processed samples exhibited more or less deflection when compared to untempered modules that had not been processed through the glass heating stage.

Table 2 - Load Testing Results (Instron Machine)

Test #	Tempering	Max Load (N)	Time (s)	Deflection (mm)	Load at Fracture (N)	Fracture Deflection (mm)	Time at Fracture (s)
SAMPLE10	Untempered w/TCO #10/Back Glass #10	999.381	181.8	3.02			
SAMPLE10b	Untempered w/TCO #10/Back Glass #10	2513.558	413	6.87	2513.56	6.87	413
SAMPLE09	Untempered	501.529	391	1.50			
SAMPLE11	Untempered	501.803	462	1.57			
SAMPLE07	Untempered	501.418	391	1.46			
SAMPLE06	Untempered	501.758	391	1.49			
SAMPLE08	Untempered	502.948	400	1.56			
SAMPLE02UT	Untempered	502.227	390	1.42			
SAMPLE01UT	Untempered	500.3	390	1.45			
SAMPLE02T	Tempered/Processed #2/ack Glass #4	503.09	400	1.59			
SAMPLE02TF	Tempered/Processed #2/Back Glass #4	3604.043	545	9.05	3604.04	9.02	541.8
SAMPLE01T	Tempered/Processed #1/Back Glass #3	501.491	400	1.54			
SAMPLE01TF	Tempered/Processed #1/Back Glass #3	4030.009	626	10	4018.19	10	617

An untempered/unprocessed sample was also loaded to fracture with the resulting peak load at 2514 N. The tempered/processed samples exhibited no loss in strength by being exposed to the glass heating stage. The results are shown below in Figure 12 and Figure 13.

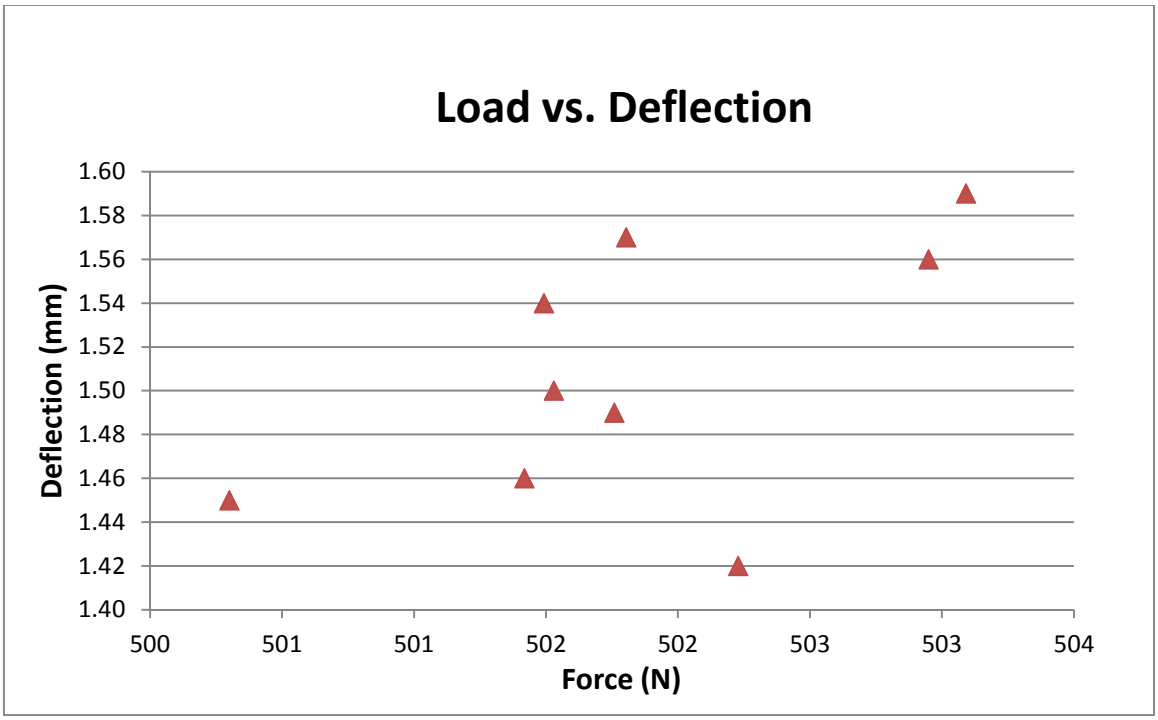

Figure 12 - Load vs. Deflection

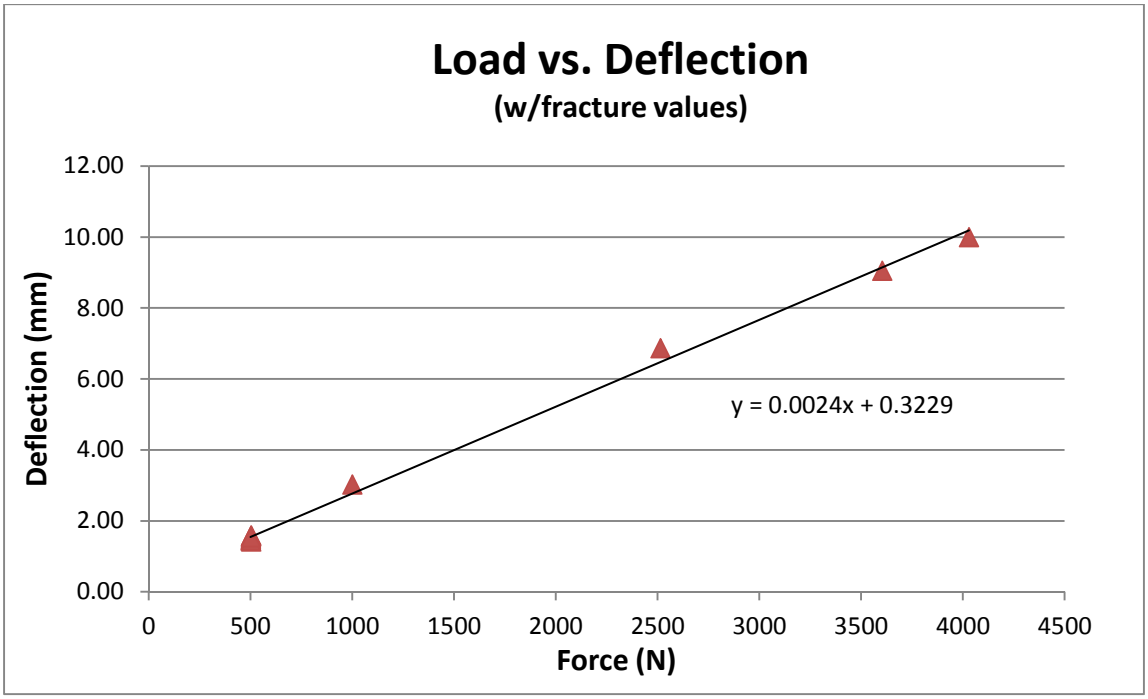

Figure 13 - Load vs. Deflection (with fracture values)

Additional Instron load testing was performed in July 2014 on three 3 mm TEC10 glass plates. The plates were loaded at the center to 500 N and held in place for 5 minutes, Aluminum supports were placed on the ends. The average deflection for the 3 mm plates was 6.44 mm. The testing configuration is shown in Figure 14.

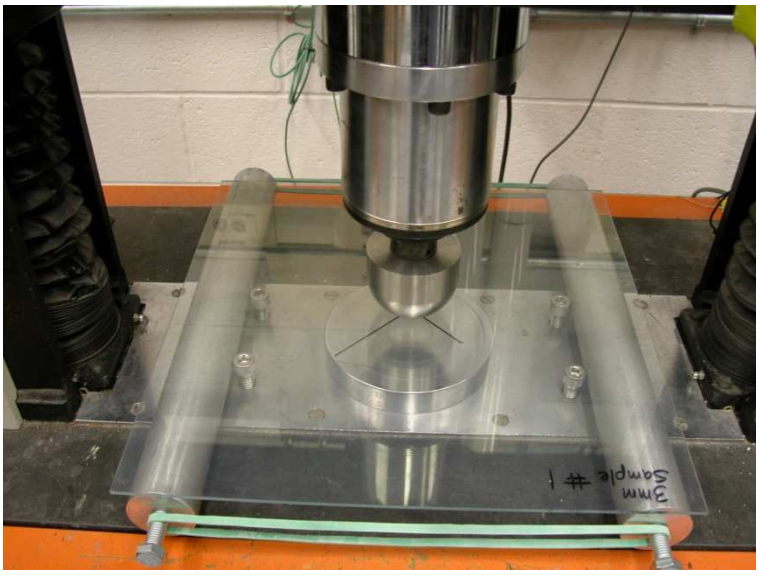

Figure 14 – 3mm TEC10 Load Testing Configuration

Distributed load tests for seven 6 mm modules and three 3 mm TEC10 glass plates were performed utilizing a 2" diameter Aluminum rod placed across the modules with the crosshead of the Instron machine place at the center of the Aluminum rod. 2" Aluminum bars to provide support were placed at 1.125" from the edge of the modules. The average deflection for the 6 mm modules was 1.5 mm. One 6 mm module was loaded to fracture with the resulting peak load at 4139 N and maximum deflection of 9.78 mm. The back glass cracked in tension, however the top glass in compression, exhibited no cracking.

For the 3 mm TEC10 glass plates, the average deflection was 6.07 mm. The configuration is shown below in Figure 15.

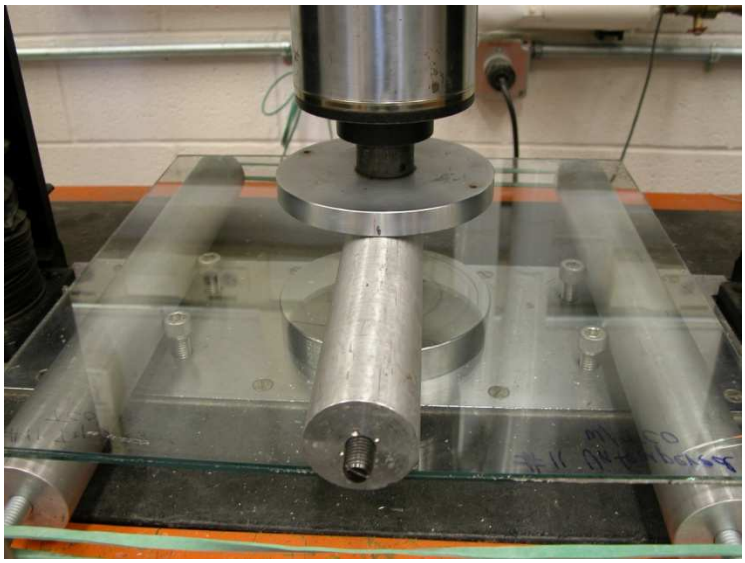

Figure 15 – Distributed Load Testing Configuration

The compilations of loading results comparing the calculated and experimental results are shown in Table 3.

Table 3 – Summary of Calculated and Experimental Maximum Deflection Results

	Deflection (mm)
Beam theory (6.49 mm, assumes acting as a single beam)	0.696
Beam theory (3 mm, assumes two beams acting separately)	3.51
Experimental Tests (6.49 mm module)	1.25

4.2 Mechanical Loading

The testing followed the requirements set forth in the IEEE 1262 standard as specified in section 5.11 Mechanical Loading Tests. The module should be mounted to a test structure that simulates installation. The module should then be instrumented and monitored throughout the test to detect any open circuits or ground faults during the test. An essentially uniform load of 2400 Pa should be applied normal to the module surface and left in place for 30 minutes. The

load should be removed and reapplied to the opposite surface for 30 minutes. These two loadings should be repeated for three cycles. [IEEE 1262].

In order for the module to successfully pass the mechanical loading requirement, the modules should not have exhibited either open or short-circuit conditions during the test. In addition, the module must pass visual inspection and electrical performance tests. The visual inspection and electrical performance requirements are referenced in Appendix C. In this study, the tests were performed on modules that did not contain applied thin film deposition of CdS and CdTe. Since the applied thin film deposition of CdS and CdTe were considered negligible for stress analysis purposes, no electrical performance testing was performed.

4.3 Hail Impact Testing

The testing followed the requirements set forth in the IEEE 1262 standard as called out in section 5.14. This test should be performed in accordance with ASTM E 1038-93. The modules should be subjected to the impact normal to the surface of 25.4 mm (1 in.) diameter ice balls traveling at an impact velocity of 23.2 m/s (52 mi/h). At least 10 of the test modules' most sensitive points should be selected for impact. The candidate points selected should include (where applicable) the following:

a) Corners and center points of cells

b) Corners and edges of the module inside the frame, if any

c) Point(s) directly near bypass diode(s) if installed

d) Soldered or bonded metallic interconnects between cells, if present.

The module is required to pass the visual inspection and electrical-performance tests.

The hail impact testing was performed by the Arizona State University (ASU) Photovoltaics Testing Laboratory in Mesa, Arizona. Three critical areas for impact were chosen

which includes a center location, edge location and corner location. Testing standards required for ice balls to be 25 mm in diameter impacting the module surface at 22.04 -24.36 m/s. Two PV modules were sent for hail impact testing. Sample #1 (Tempered/Processed) passed the hail test with the following velocities performed at the areas of impact: corner – 23.3 m/s, edge – 23.5 m/s, center – 24.2 m/s. The second sample sent for testing, Sample #2 (Tempered/Processed) passed hail test with the following velocities performed at the areas of impact: corner – 23.5 m/s, edge – 23.3 m/s, center – 24.2 m/s. Hail ball weight: 8.2 g, hail ball diameter: 25.65 mm (1.01").

The hail impact testing configuration is shown in Figure 16.

Figure 16 – Hail Impact Testing Configuration

A pre-test photograph of the sample is shown in Figure 17.

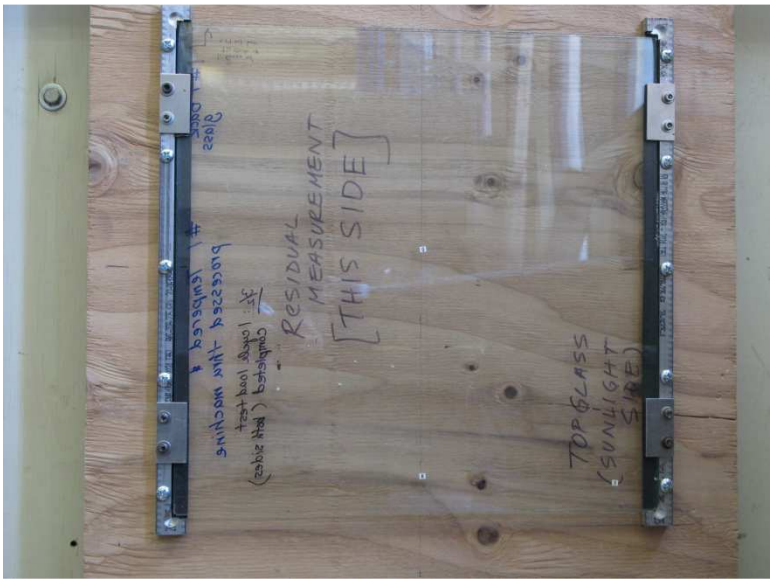

Figure 17 – Pre-test Sample

A post-test photograph of the sample is shown in Figure 18.

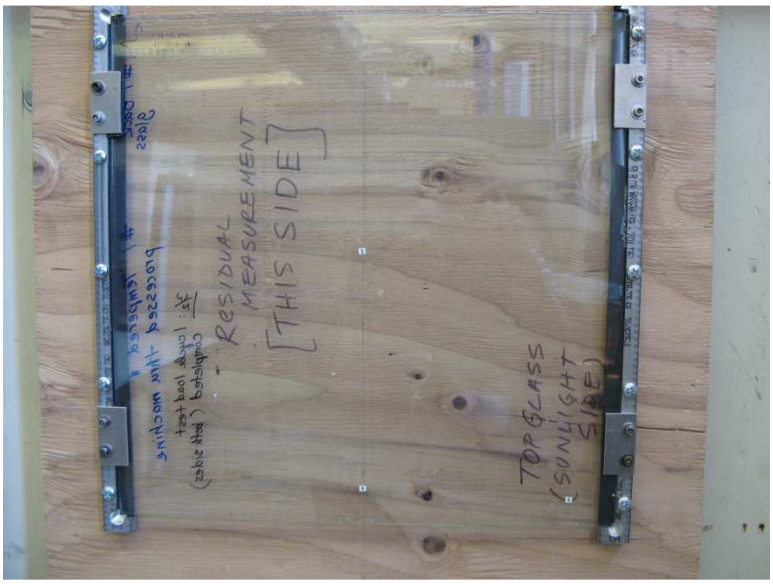

Figure 18 – Post-test Sample

4.4 Residual Stress Measurement

A residual stress measurement was performed by Strainoptics, Inc. of North Wales, PA in order to determine the remaining level of residual stresses in the tempered PV module. The

residual stresses are measured by using a Laser GASP (Grazing Angle Surface Polarimeter). The GASP surface polarimeter is based on photoelastic test methods, using light rays traveling along the glass surface. An operator places a drop of index matching fluid on the tin side of soda-lime float glass to ensure optical contact. The instrument is placed with its prism surfaces on the fluid, such that light travels through the entrance prism at a critical angle (i_c), enters the top surface of the glass and propagates parallel to the surface for a distance before emerging at a critical angle into the exit prism and up toward the eyepiece. [Strainoptics, Inc.]

The measurement followed the requirements set forth in ASTM C1048, "Standard Specification for Heat-Treated Flat Glass—Kind HS, Kind FT Coated and Uncoated Glass". The stress measurement was performed in five different locations on the PV module. These locations are designated as: 1) A, 2) B, 3) C, 4) D and 5) E and are shown in Figure 19. The average of the ten readings resulted in surface stress of 2718 psi. The item could not be described by ASTM C1048 as either Kind HS or Kind FT. The residual stress in tempered glass is approximately 10,000 psi and the processing reduces the residual stress to 2,718 psi. The tempered glass was not measured "as received" prior to being fabricated into a PV module.

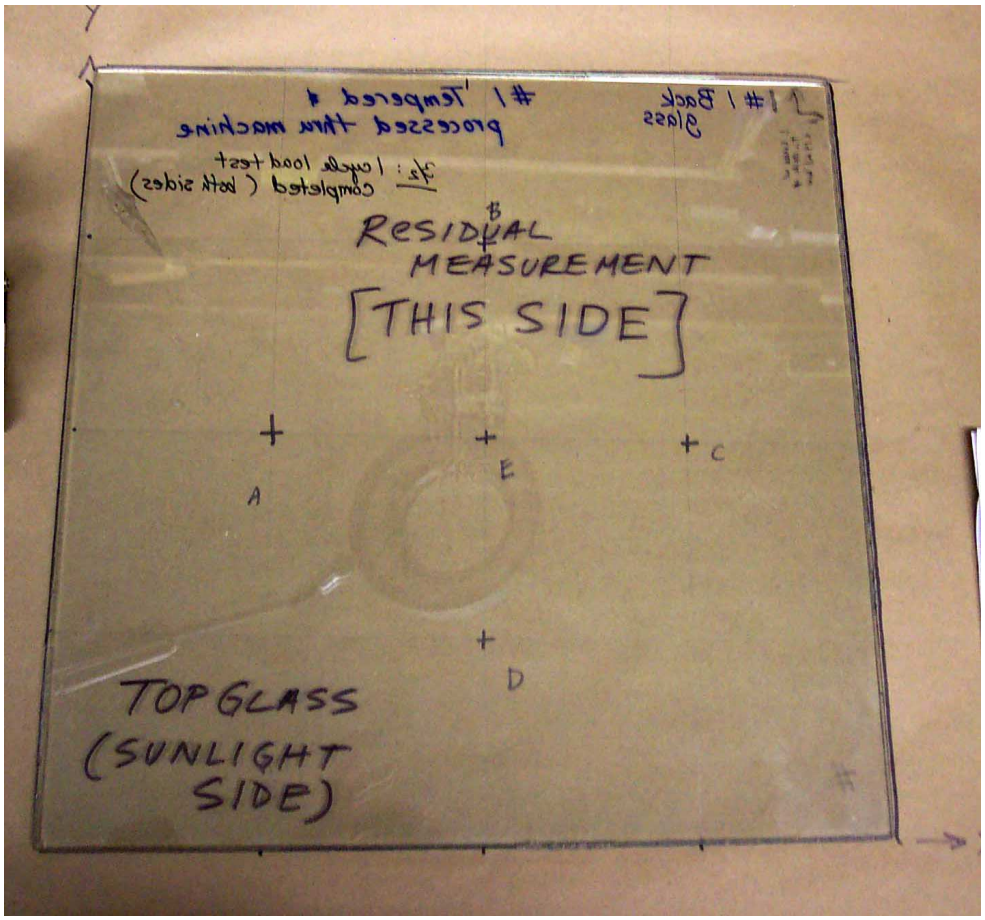

Figure 19 – Hail Impact Configuration

Chapter 5: CONCLUSIONS AND RECOMMENDATIONS

5.1 Conclusions

From the research, general topics and information in the literature has been investigated. This information has been utilized in this thesis to complete an accurate characterization of the mechanical loading characteristics and stress in the composite PV modules. The theoretical mathematical model defined mechanical behavior within the PV module. The vibration analysis provided the determination on whether the hail impact can be modeled statically or dynamically. As referenced in Norville's research, if the composite plate is modeled statically as one beam, the deflection will be significantly lower as compared to the modeling of two separate beams in bending.

The processing conditions of the glass plates in the heating stage contribute to the structural integrity of the module. The heating of the top tempered glass during processing decreases the residual stress in the composite module. The mechanical load testing and residual stress measurement provided information to understand the effects of temper loss and whether the module exhibited a loss in strength. The results showed that the samples met the requirements after being exposed to the glass heating stage.

For the physical testing of the PV composite modules, the experimental design had several goals. One goal was to measure the amount of deflection by using sandbags as the simulated distributed load. For the 16" x 16" modules, the deflection measurements were taken by a digital micrometer prior to and after loading. The deflection measurements would determine if the modules would pass the static loading tests to successfully complete the qualification testing as specified by the IEEE Standard 1262.

A second goal of the physical testing of the PV composite modules was to perform concentrated center loading to measure the amount of deflection. This was performed using an Instron machine. Load vs. deflection curves show the amount of deflection for the various untempered and tempered samples. These results were compared to mathematical models using both plate and beam theory for maximum deflection.

From the limited number of samples tested, the following conclusions can be drawn: 1) the PV module successfully passed the static loading tests, 2) the maximum measured deflection correlated to the mathematical equation for beam theory which provides justification that the PV module exhibits behavior between one and two beams, and 3) in the analysis of the hail impact loading, the PV was determined to act statically not dynamically.

The EVA encapsulant may contribute to the bending capacity of the overall PV module through load-induced flexural stresses. However, its major functions consist of bonding the glass plates, maintaining spacing, and transferring some fraction of the horizontal shear force between the glass plates.

5.2 Future work and recommendations

The results from this study provided initial data that the loss of the residual stress during processing allowed the modules to meet the requirements. This was subsequently tested on production size modules 2' x 4' and found to be true. The module may be overdesigned. There is a potential to reduce glass thickness, in order to reduce the cost of the modules.

All testing for this research project was done at ambient temperature. For future work, the tests can be performed at elevated temperatures to understand the behavior of the photovoltaic module.

REFERENCES

1. Beer, F.P, and Johnston, E.R., Mechanics of Materials, Second Edition, McGraw-Hill, Inc., 1992.
2. Behr, R.A., Minor, J.E., Norville, H.S. (1993), "Structural Behavior of Architectural Laminated Glass" *J. Struct. Engrg.,* Vol. 119, No. 1, pp. 202-222.
3. Behr, R.A., Kremer, P.A., (1996), "Performance of Laminated Glass Units under Simulated Windborne Debris Impacts." *J. Arch. Engrg.,* Vol. 2, No. 3, pp. 95-99.
4. Craig, R.R., Jr., Structural Dynamics – An Introduction to Computer Methods, Second Jon Wiley & Sons, 1992.
5. Flocker, F.W., and Dharani, L.R. (1997), "Stresses in Laminated Glass Subject To Low Velocity Impact", *Engineering Structures*, Vol. 19, No. 10, pp. 851-856
6. Flocker, F.W., and Dharani, L.R. (1997), "Modelling Fracture in Laminated Architectureal Glass Subject to Low Velocity Impact", *J. Mater. Sci*, Vol. 32, pp. 2587-2594.
7. Gere, J.M., Mechanics of Materials, Sixth Edition, Brooks/Cole, 2004.
8. GTM Research, April 2014, *PV Pulse*
9. Hooper, J.A., (1973), "On the Bending of Architectural Laminated Glass" *Int. J. Mech Sci.,* Vol. 15 pp. 309-323.
10. Institute of Electrical and Electronics Engineers (IEEE) 1262 - *IEEE Recommended Practice for Qualification of Photovoltaic (PV) Modules*
11. IEC 61215 - *"Design Qualification and Type Approval for Crystalline Silicon Terrestrial Photovoltaic Modules"*
12. IEC 61646 - *"Thin Film Torrential Photovoltaic (PV) Modules - Design Qualification and Type Approval"*
13. Jäger-Waldau, Arnulf, Joint Research Centre, *PV Status Report*, 2013
14. Kempe, M.D., Jorgensen, G.J., Terwilliger, K.M., McMahon, T.J., Kennedy, C.E., Borek, T.T., "Ethylene-Vinyl Acetate Potential Problems for Photovoltaic Packaging", Conference Paper, May 2006.
15. Kim, H., and Kedward, K., (2000), "Experimental Measurement and Numerical Prediction of Hail Ice Impact on Composite Panels" *AIAA Journal,* Vol. 38, No. 7, pp. 1278-1288.
16. Knight, C.G., Swain, M.V., and Chaudhri, M.M., (1977), "Impact of Small Steel Spheres on Glass Surfaces", *J. Mater. Sci*, Vol. 12, No. 8, pp. 1573-1586.
17. Norville, H. S., King, K. W., and Swofford, J. L., (1998), "Behavior and Strength of Laminated Glass." *J. Engrg. Mech.*, ASCE, Vol. 124, No. 1, pp. 46–53.
18. Norville, H. S., Minor, J.E., (1985), "Strength of Weathered Window Glass" *Am. Ceram. Soc. Bull.,* Vol. 64, No. 11, pp. 1467-1470.
19. Norville, H. S., Bove, P.M., Sheridan, D.L., Lawrence, S.L., (1992), "Strength of New Heat Treated Window Glass Lites and Laminated Glass Units" *J. Struct. Engrg.,* Vol. 119, No. 3, pp. 891-901.
20. Sampath, W.S., Barth, K., and Enzenroth, R.A, "Stability, Yield and Efficiency of CdS/CdTe Devices", Final Report for Thin Film Partnership Program, September 2001 – September 2004.
21. Strainoptics, Inc., "GASP® Instruments for measuring surface stresses in tempered, heat-strengthened, and annealed glass", Bulletin GSP-0112, 2011.

22. Timoshenko, S. and Woinowsky-Krieger, S., Theory of Plates and Shells, Second Edition, McGraw-Hill, Inc., 1987.
23. Troshin, N. N., and Yaster, V.V., (1988), "Calculation of Resistance of Flat Glass to the Action of Hail" *Glass and Ceramics (English Translation of Steklo i Keramika)*, Vol. 45, No. 9-10, pp. 372-374.
24. Vallabhan, C. V. G., Minor, J.E., and Nagalla, S.R., (1987), "Stesses in Layered Glass Units and Monolithic Glass Plates" *J. Struct. Engrg,* Vol. 113, No. 1, pp. 36-43.
25. Vallabhan, C. V. G., Das, and Ramasamudra, M., (1992), "Properties of PVB Interlayer Used in Laminated Glass" *J. Mater. in Civil Engrg.,* Vol. 4, No. 1, pp. 71-76.
26. Vallabhan, C. V. G., Das, Y. C., Magdi, M., Asik, M., and Bailey, J. R., (1993), "Analysis of Laminated Glass Units." *J. Struct. Engrg,* Vol. 119, No. 5, 1572–1585.
27. Van Duser, A., Jagota, A., Bennison, S., (1999), "Analysis of Glass/Polyvinyl Butyral Laminates Subjected to Uniform Pressure", *J. Engrg. Mech.*, Vol. 125, No. 4, pp. 435-442.
28. IEEE 1262 *"IEEE Recommended Practice for Qualification of Photovoltaic Modules"(1995)*
29. ASTM C1048 "Standard Specification for Heat-Treated Flat Glass – Kind HS, Kind FT Coated and Uncoated Glass."

APPENDIX A

List of calculations to obtain mechanical loading characteristics:

In performing the mathematical analysis, several classic mechanics of materials equations are utilized. Equation 1 will obtain the maximum normal stress, assuming Hooke's law applies where the normal stress (σ_y) does not exceed the yield strength (σ_y). Equation 2 will obtain the maximum shearing stress in a given section of a narrow rectangular beam. Equation 3 will obtain strain values within the composite layers.

$$\sigma = \frac{Mc}{I} \quad (1) \qquad \tau_{\max} = \frac{3V}{2A} \quad (2) \qquad \varepsilon = \frac{\sigma}{E} \quad (3)$$

For plate deflection calculations, the Navier solution [Timoshenko, 1987] for a single load concentrated at any point that is simply supported was used to estimate the amount of deflection. In the case for a square plate, the equation for maximum deflection is:

$$w_{\max} = \frac{0.01121Pa^2}{D} \quad (4)$$

Where P=concentrated load, a=plate length and D=flexural rigidity. For the tested photovoltaic modules, P=112 lb_f (500 N), a=16 in. (406 mm) and D=15,173 in-lbs. Flexural rigidity is defined as:

$$D = \frac{Eh^3}{12(1-\upsilon^2)} \quad (5)$$

Where E=modulus of elasticity, h=plate thickness and υ=Poisson's ratio. For the tested photovoltaic modules, E=68.9 GPa (10 x 10^6 psi), h=6.49 mm (0.255 in.), and υ=0.23

The calculated maximum deflection ($w_{\max}$) utilizing plate theory for the 6.49 mm photovoltaic modules was 0.539 mm (0.0212 in.).

Similar calculations were performed for a photovoltaic module with thickness of 3 mm (0.118 in.). The calculated maximum deflection ($w_{\max}$) utilizing plate theory for the 3 mm photovoltaic modules was 5.449 mm (0.2145 in.). These values did not mirror the tested deflection results of 1.5 mm. So, it was determined that the photovoltaic module did not behave as a plate.

The photovoltaic module was next analyzed using beam theory for a beam simply supported at end and a concentrated load at the center [Gere, 2004] to estimate the amount of deflection. The equation for maximum deflection is:

$$\delta_{\max} = \frac{PL^3}{48EI} \quad (6)$$

Where P=concentrated load, L=plate length, E=modulus of elasticity, and I=moment of inertia. For the tested photovoltaic modules, P=112 lb_f (500 N), L=16 in. (406 mm), E=68.9 GPa (10 x 10^6 psi). For the moment of inertia:

$$I = \frac{bh^3}{12} \quad (7)$$

Where b=width, h=height. For the tested photovoltaic modules, b=16 in. (406 mm), and h=6.49 mm (0.255 in.). I=0.0221 in^4. The calculated maximum deflection ($\delta_{\max}$) utilizing beam theory for the 6.49 mm photovoltaic modules was 1.098 mm (0.043 in.). However, this calculation did not account for the supported ends in the testing configuration of the photovoltaic modules. So, calculating L=13.75 in. in equation (6) results in a calculated maximum deflection ($\delta_{\max}$) utilizing beam theory for the 6.49 mm photovoltaic modules of 0.879 mm (0.0346 in.). This deflection value corresponds more closely to the experimentally tested results of 1.50 mm. The contribution of the testing supports and the effect of the EVA were calculated. These results contributed minimally to the overall deflection.

APPENDIX B

List of calculations to obtain calculated impact force of hail:

Average impact diameter – 7.75 mm

Average impact velocity – 22.9 m/s

Nominal diameter – 25 mm

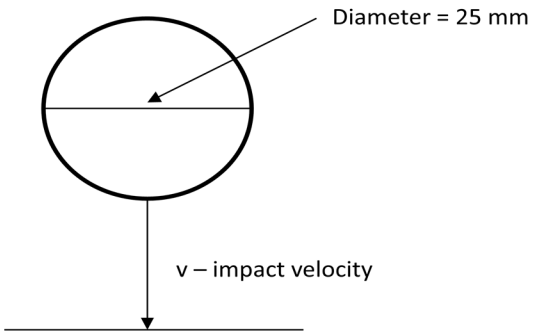

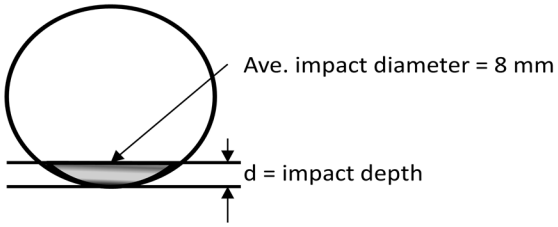

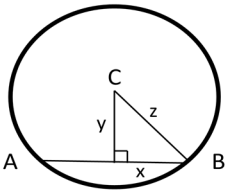

x = 4 mm

z = 12.5 mm (radius)

$x^2 + y^2 = z^2$

$y^2 = z^2 - x^2$

$y = z^2 - x^2$

$y = \sqrt{z^2 - x^2}$

$y = \sqrt{12.5^2 - 4^2}$

y = 11.84 mm

d = z - y

d = 12.5 mm – 11.84 mm

d = 0.6573 mm

So, assuming constant acceleration

$v = at + v_0$ (8) Solving for time (t): $t = \frac{v - v_0^2}{a}$ (9),

$v^2 = v_0^2 + 2a(x - x_0)$ (10) Solving for acceleration (a) in Eqn. (10):

$a = \frac{v^2 - v_0^2}{2x}$ $a = \frac{22.9 m/s^2}{2(0.6573 \times 10^{-3} m)}$ $a = 398{,}912 \frac{m}{s^2}$

$$t = \frac{22.9 m/s^2}{398{,}912 \frac{m}{s^2}} \qquad t = 57.4 \mu s$$

Equation for density: $\rho = \frac{m}{V}$ (11)

Solving for mass (m) in Eqn. (11): $m = V\rho$ (12)

Using density value for ice = 916.8 kg/m^3 , Volume of sphere: $V_{sphere} = \frac{4}{3}\pi r^3$

Inputting into Eqn. (12): $m = \left(\frac{4}{3}\pi r^3\right)\left(916.8 \frac{kg}{m^3}\right)$, $m = \left(\frac{4}{3}\pi\left(12.5x10^{-3}\, m\right)^3\right)\left(916.8 \frac{kg}{m^3}\right)$,

$m = 0.0075kg$

Equation for Force (F) $F = ma$ (13) $F = (0.0075kg)(398{,}912 m/s)$

$F = 2991.84N(672lb_f)$

APPENDIX C

Test requirements from IEEE 1262:

5.1 Visual Inspection Procedure

This procedure provides guidelines for obtaining the baseline, intermediate, and final visual inspection required to identify and determine any physical changes or defects in module construction at the beginning and after the completion of each required test as specified in clause 4.

Purpose:

To determine the physical condition of the module and to document this condition for comparison with future inspections.

Procedure:

Modules should be visually inspected without magnification for any observed defects or abnormalities, which should be documented with appropriate sketches or photographs to show the location of any defects. Inspectors should look for but not be limited to the following:

a) Poor workmanship, shipping damage, mechanical mounting defects
b) Cracking, shrinkage, or distortion of a polymeric material used for electrical insulation or isolation.
    1. Failure of adhesive bonds
    2. Tacky surfaces of plastic modules
c) Corrosion of fasteners, mechanical members, or electrical circuit elements.
    1. Discoloration of the superstrate, encapsulating material, or active PV device surfaces.
    2. Voids in, or visible corrosion of any thin-film layers of the active circuitry of the module.
d) Bubbles, delaminations, or the presence of foreign material.
e) Mechanical distortion, buckling, or evidence of yielding.
f) Broken, cracked or torn external surfaces
g) Broken cells or cracked cells
h) Cells touching one another or the frame
i) Terminals not bonded to the module or terminal box
j) Faulty interconnects or joints
k) Any other condition that may affect performance

Requirements:

If a module exhibits any major defect during any of the visual inspections, it is considered to have failed the qualification test. Major visual defects are defined as:

a) Broken or cracked window
b) Voids in, or visible corrosion of any thin-film layers of the electrical circuit of the module, extending over more than 10% of the active area of the cell.

c) Bubbles or delamination forming a continuous path between any part of the electrical circuit and the edge of the module.
d) Loss of mechanical integrity, to the extent that the installation and/or operation of the module would be impaired.

If a module exhibits initial defects that are not due to the manufacturing process, a new module may be substituted before beginning the test sequence.

APPENDIX D

TEST REPORT

APRIL 5, 2007

TO

W. S. SAMPATH
COLORADO STATE UNIVERSITY
ENG. RES. CENTER B120
200 LAKE ST.
FT. COLLINS, CO
80523-1320

STRAINOPTICS SO# 3431

SUBMITTED
BY
TIM WILSON
ENGINEERING SERVICES MANAGER

STRAINOPTICS, INC.
108 W. MONTGOMERY AVE.
NORTH WALES, PA 19454
(215) 661-0100
www.strainoptics.com

1. **TEST DATE AND LOCATION:**
   a. April 4, 2007, Strainoptics, Inc., North Wales, PA

2. **OBJECTIVE:**
   a. Provide surface stress measurements for one laminated flat architectural glass sample per ASTM C1048, "Standard Specification for Heat-Treated Flat Glass—Kind HS, Kind FT Coated and Uncoated Glass".

3. **TEST ITEMS:**
   a. One clear laminated flat glass sample 16.5" x 16.5" x 0.24"
   b. See Figure 1.

4. **PROCEDURE:**
   a. A calibrated Laser GASP serial number 678 was used to measure surface stress in accordance with ASTM C1048.
   b. For traceable calibration of GASP 678 see ASTM Designations C1377, "STANDARD TEST METHOD FOR CALIBRATION OF SURFACE STRESS MEASURING DEVICES".
   c. Additional information regarding ASTM standards can be found at www.astm.org.

5. **RESULTS:**

See Table 4

6. CONCLUSIONS:

The average of the ten readings resulted in surface stress of 2718 psi. The item could not be described by C1048 as either Kind HS or Kind FT.

Table 4

MEASUREMENT LOCATION	STRESS (psi)
Ax	2467
Ay	2847
Bx	2718
By	2718
Cx	1984
Cy	2718
Dx	2847
Dy	2718

Ex	2978
Ey	2978
AVERAGE	2718

APPENDIX E

List of materials/equipment used for testing:

1. Ethylene Vinyl Acetate (EVA)
    - Solar cell encapsulants modified EVA
    - Project #: 50921
    - Formulation: 15420P/VF, area: 97 ft^2, length: 30 LF, thickness: 0.018 inch.
    - 9 month shelf life, ship date: 22 March 2006
    - Specialized Technology Resources Inc., 10 Water St., Enfield, CT 06082

2. Laminator
    - Dimension II
    - Model LM-404 Solar Module Laminator
        - Vacuum at 24 in Hg upper chamber
        - 1.8 torr in lower chamber
        - 220 VAC, 50/60 Hz, 1 phase, 15 Amps, 3 kW
    - Astropower, Inc., Newark DE

3. Instron Machine
    - MTS Instron 1125
        - Calibrated 3/29/2007 0.01 – 500 mm/min
        - up to 200 mm of travel
    - Software: Testworks 4.0 by MTS

LIST OF ABBREVIATIONS

Cadmium Chloride	$CdCl_2$
Cadmium Sulfide	CdS
Cadmium Telluride	CdTe
Colorado State University	CSU
Ethylene Vinyl Acetate	EVA
Laminated Glass	LG
Los Alamos National Laboratory	LANL
Materials Engineering Laboratory	MEL
National Renewable Energy Laboratory	NREL
Photovoltaics	PV
Polyvinyl Butyral	PVB
Transparent Conductive Oxide	TCO